Supplement of Hydrol. Earth Syst. Sci., 26, 1745–1754, 2022
https://doi.org/10.5194/hess-26-1745-2022-supplement

Hydrology and Earth System Sciences
Open Access
EGU

Supplement of

Testing a maximum evaporation theory over saturated land: implications for potential evaporation estimation

Zhuoyi Tu et al.

Correspondence to: Yuting Yang (yuting_yang@tsinghua.edu.cn)

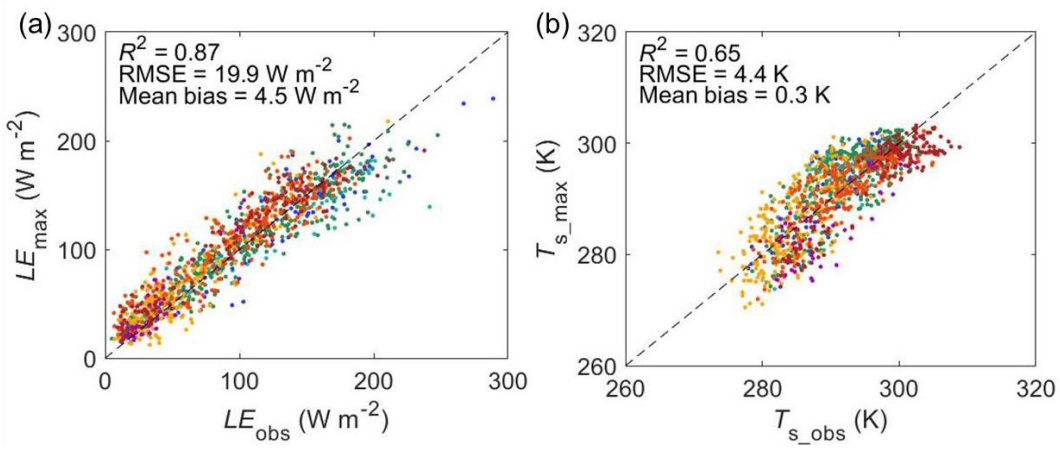

Figure S1. Validation of LE and T_s estimated using the maximum evaporation approach at the selected site-days where the energy balance closure of the flux site measurements is achieved by using the Bowen ratio approach (Twine et al., 2000). The colors represent different biome types (as provided in Figure 1). The dashed black lines indicate the 1:1 line.

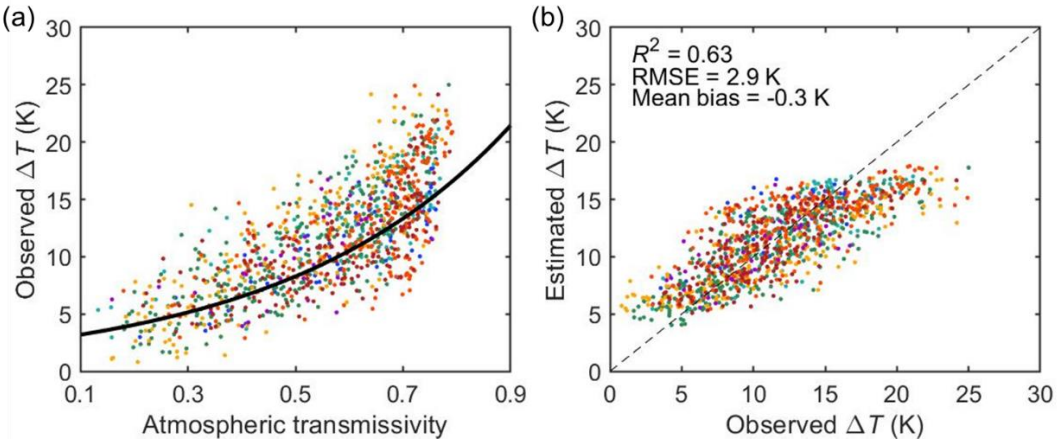

Figure S2. Estimation of temperature difference between the surface and the effective radiating height of the atmosphere (ΔT). (a) Relationship between ΔT and atmospheric transmissivity (τ) across all 1128 non-water-limited site-days. The thick black curve represents the ΔT-τ relationship obtained over global ocean surfaces in Yang and Roderick (2019) (i.e., $\Delta T = 2.52\exp(2.38\tau) + 0.035|lat|$) and the colored dots/lines represent different biome types (legend provided in Figure 1). (b) Comparison between observed ΔT and estimated ΔT using Eq. (5) in Sect. 2.2.

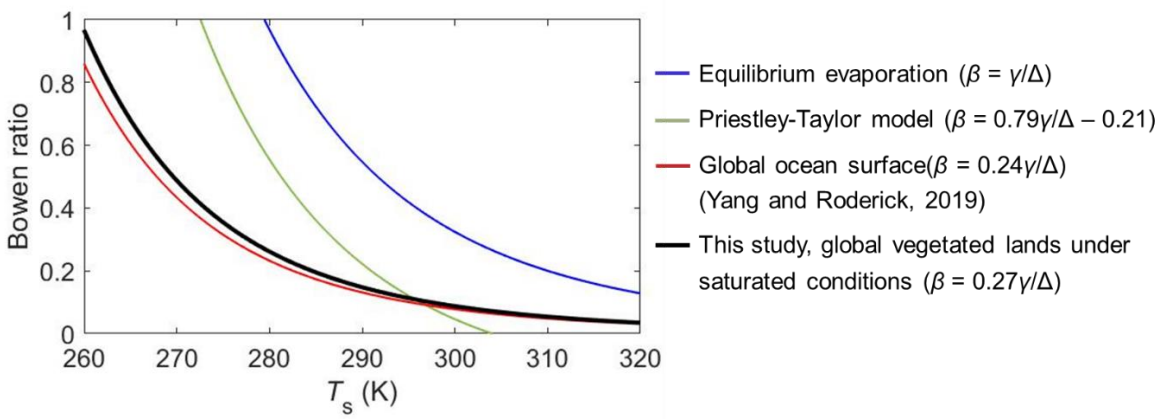

Figure S3. Relationships between the Bowen ratio (β) and surface temperature (T_s).

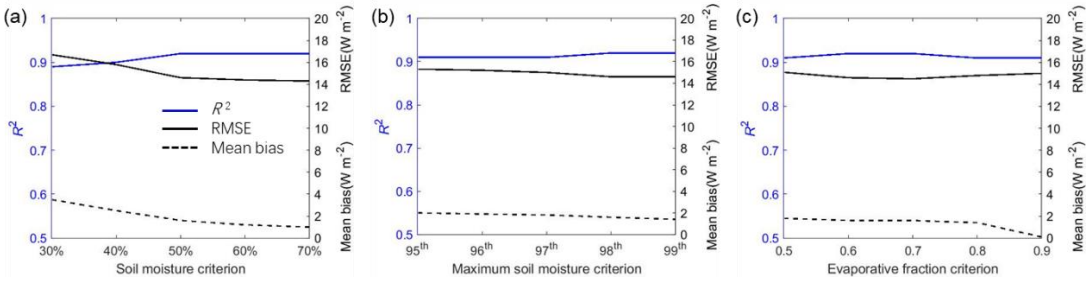

Figure S4. The performance of the maximum evaporation model in estimating *LE* with varying selection criteria of unstressed evaporation observations. (a) The soil moisture criterion varies from 30% to 70%, (b) the Maximum soil moisture criterion varies from 95th to 99th percentile and (c) the evaporative fraction criterion varies from 0.5 to 0.9.

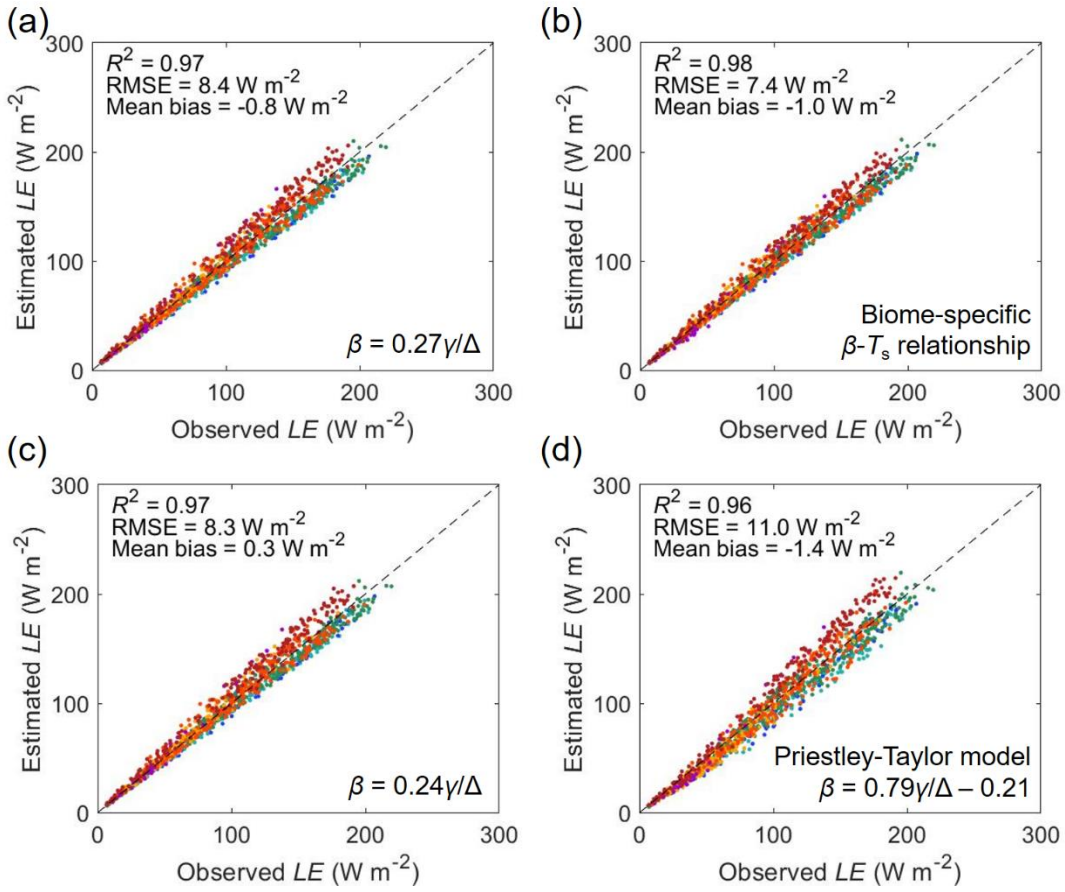

Figure S5. Estimation of *LE* using observed net radiation (per Eq. (1)). Comparison of estimated *LE* using observed net radiation with four different β-T_s relationships. (a) Generic land β-T_s relationship ($\beta = 0.27\gamma/\Delta$), (b) Biome-specific β-T_s relationships (per Figure 2), (c) Ocean surface β-T_s relationship ($\beta = 0.24\gamma/\Delta$) and (d) the Priestley-Taylor model ($\beta = 0.79\gamma/\Delta - 0.21$). The colors represent different biome types (legend provided in Figure 1). The dashed black lines indicate the 1:1 line.

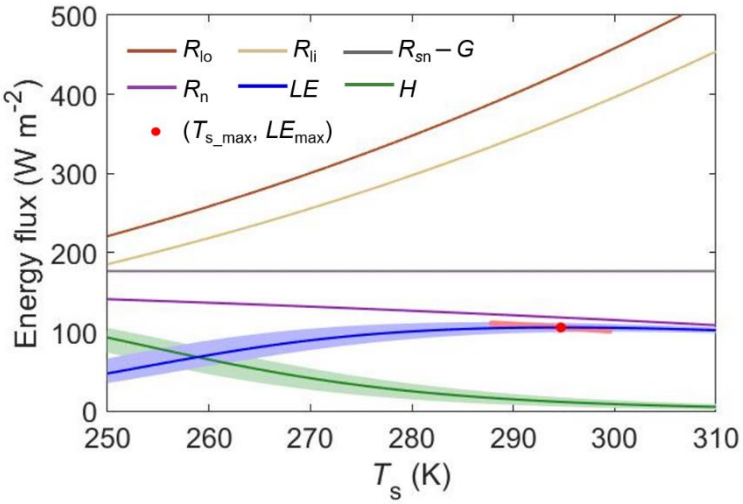

Figure S6. Variations of energy fluxes with T_s within the maximum evaporation framework with different β-T_s relationships. In this calculation, the coefficient of the β-T_s relationship (i.e., m) varies from 0.18 to 0.36 and all other forcings are the same as those in Figure 3. The solid line represents the case when $\beta = 0.27\gamma/\Delta$ and the shadows represent the range of all cases for m changing between 0.18 and 0.36. The red dots show the location of LE_{max} when $\beta = 0.27\gamma/\Delta$ and the short red line shows the locations of LE_{max} when m changes between 0.18 and 0.36.

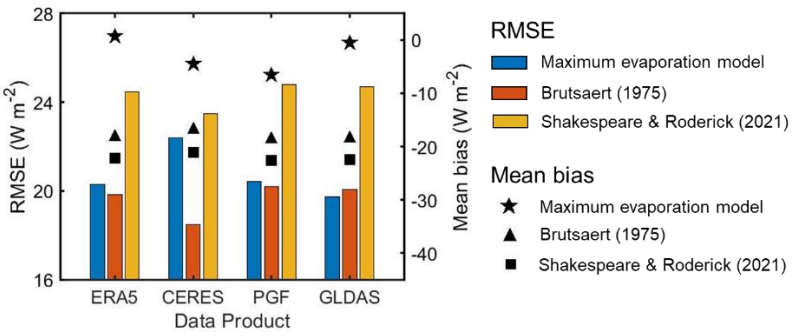

Figure S7. Comparison of three model performance in estimating incoming longwave radiation validated against four global products under wet conditions across the globe (the wet conditions are determined following Milly and Dunne, 2016). The three compared models include the maximum evaporation model in this study, the Brutsaert model (1975) and the Shakespeare and Roderick model (2021). The four global products include ERA5 (1979-2019; Hersbach et al., 2019), CERES (2001-2016; Kato et al., 2018), the Princeton global forcing dataset (PGF, 1979-2010; Sheffield et al., 2006) and the GLDAS global forcing dataset (1979-2014; Rodell et al., 2004).

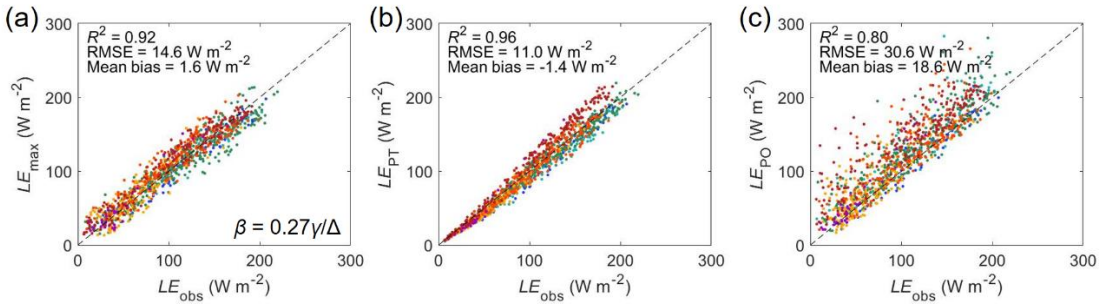

Figure S8. Estimation of *LE* at unstressed site-days. (a) The maximum evaporation model, (b) The Priestley-Taylor model, (c) The Open Water Penman model. The colors represent different biome types (as provided in Figure 1). The dashed black lines indicate the 1:1 line.

Table S1. Descriptions of the flux sites used in this study including site number (Site Num), site identifier (Site ID), latitude (Lat), Longitude (Lon), biome type and number of selected days (Site-days).

Site Num	Site ID	Lat (°N)	Lon (°E)	Biome Type	Site-days
1	AU-ASM	-22.28	133.25	Savanna	2
2	AU-Ade	-13.08	131.12	Savanna	5
3	AU-Cpr	-34.00	140.59	Savanna	13
4	AU-Cum	-33.62	150.72	Broadleaf forest	12
5	AU-DaP	-14.06	131.32	Grassland	22
6	AU-DaS	-14.16	131.39	Savanna	24
7	AU-Dry	-15.26	132.37	Savanna	34
8	AU-Emr	-23.86	148.47	Grassland	14
9	AU-Fog	-12.55	131.31	Wetland	16
10	AU-GWW	-30.19	120.65	Savanna	8
11	AU-Gin	-31.38	115.71	Savanna	16
12	AU-How	-12.49	131.15	Savanna	28
13	AU-Lox	-34.47	140.66	Broadleaf forest	6
14	AU-RDF	-14.56	132.48	Savanna	4
15	AU-Rig	-36.65	145.58	Grassland	4
16	AU-Stp	-17.15	133.35	Grassland	4
17	AU-TTE	-22.29	133.64	Grassland	1
18	AU-Tum	-35.66	148.15	Broadleaf forest	12
19	AU-Wac	-37.43	145.19	Broadleaf forest	3
20	AU-Whr	-36.67	145.03	Broadleaf forest	12
21	AU-Wom	-37.42	144.09	Broadleaf forest	3
22	AU-Ync	-34.99	146.29	Grassland	13
23	BE-Lon	50.55	4.75	Cropland	5
24	BR-Sa3	-3.02	-54.97	Broadleaf forest	12
25	CA-Gro	48.22	-82.16	Needleleaf forest	1
26	CA-Qfo	49.69	-74.34	Needleleaf forest	13
27	CA-SF1	54.49	-105.82	Needleleaf forest	8
28	CA-SF2	54.25	-105.88	Needleleaf forest	10
29	CA-SF3	54.09	-106.01	Shrubland	1
30	CA-TP4	42.71	-80.36	Needleleaf forest	23
31	CA-TPD	42.64	-80.56	Broadleaf forest	10
32	CH-Cha	47.21	8.41	Grassland	8
33	CH-Fru	47.12	8.54	Grassland	10
34	CN-Cng	44.59	123.51	Grassland	14
35	CZ-wet	49.02	14.77	Wetland	13
36	DE-Geb	51.10	10.91	Cropland	36
37	DE-Hai	51.08	10.45	Broadleaf forest	22
38	DE-Kli	50.89	13.52	Cropland	11
39	DE-Lkb	49.10	13.30	Needleleaf forest	2
40	DE-Lnf	51.33	10.37	Broadleaf forest	27

41	DE-Obe	50.79	13.72	Needleleaf forest	7
42	DE-SfN	47.81	11.33	Wetland	9
43	DE-Tha	50.96	13.57	Needleleaf forest	16
44	DE-Zrk	53.88	12.89	Wetland	13
45	DK-Sor	55.49	11.64	Broadleaf forest	7
46	FI-Hyy	61.85	24.29	Needleleaf forest	5
47	FR-Gri	48.84	1.95	Cropland	10
48	FR-LBr	44.72	-0.77	Needleleaf forest	7
49	IT-BCi	40.52	14.96	Cropland	11
50	IT-CA1	42.38	12.03	Broadleaf forest	10
51	IT-CA3	42.38	12.02	Broadleaf forest	12
52	IT-Col	41.85	13.59	Broadleaf forest	22
53	IT-Isp	45.81	8.63	Broadleaf forest	13
54	IT-Lav	45.96	11.28	Needleleaf forest	25
55	IT-MBo	46.01	11.05	Grassland	21
56	IT-Noe	40.61	8.15	Shrubland	29
57	IT-Ren	46.59	11.43	Needleleaf forest	1
58	IT-SR2	43.73	10.29	Needleleaf forest	3
59	IT-SRo	43.73	10.28	Needleleaf forest	5
60	IT-Tor	45.84	7.58	Grassland	8
61	MY-PSO	2.97	102.31	Broadleaf forest	34
62	NL-Hor	52.24	5.07	Grassland	3
63	NL-Loo	52.17	5.74	Needleleaf forest	14
64	RU-Fyo	56.46	32.92	Needleleaf forest	8
65	US-AR1	36.43	-99.42	Grassland	13
66	US-AR2	36.64	-99.60	Grassland	4
67	US-ARM	36.61	-97.49	Cropland	19
68	US-CRT	41.63	-83.35	Cropland	1
69	US-GLE	41.37	-106.24	Needleleaf forest	2
70	US-Goo	34.25	-89.87	Grassland	17
71	US-MMS	39.32	-86.41	Broadleaf forest	59
72	US-Me2	44.45	-121.56	Needleleaf forest	8
73	US-NR1	40.03	-105.55	Needleleaf forest	1
74	US-Oho	41.55	-83.84	Broadleaf forest	29
75	US-SRC	31.91	-110.84	Needleleaf forest	9
76	US-SRG	31.79	-110.83	Grassland	31
77	US-SRM	31.82	-110.87	Savanna	45
78	US-Tw2	38.10	-121.64	Cropland	13
79	US-Tw3	38.12	-121.65	Cropland	14
80	US-Tw4	38.10	-121.64	Wetland	7
81	US-Var	38.41	-120.95	Grassland	34
82	US-WCr	45.81	-90.08	Broadleaf forest	10
83	US-Whs	31.74	-110.05	Shrubland	7
84	US-Wkg	31.74	-109.94	Grassland	8

85	ZA-Kru	-25.02	31.50	Savanna	8
86	ZM-Mon	-15.44	23.25	Broadleaf forest	14

Table S2. Worked example of applying the maximum evaporation model for E_P estimation (R_{si}: incoming shortwave radiation at the surface; R_{so}: outgoing shortwave radiation at the surface; R_{si_TOA}: incoming shortwave radiation at the top of the atmosphere).

Variable	Value	Source/Method
	Input	
R_{si}	200.0 W m^{-2}	Observed
R_{so}	40.0 W m^{-2}	Observed
R_{si_TOA}	300.0 W m^{-2}	Observed
lat	10.0°	Observed
ε	0.98	MOD11A1
T_s	[273.1 K, …., 313.1 K] at 0.1 K interval	Prescribed
P_{air}	101.3 kPa	Observed
	Calculation/Output	
τ	0.667	R_{si}/R_{si_TOA}
ΔT	14.2 K	Equation (5)
R_n	[100.4 W m^{-2}, …., 69.3 W m^{-2}]	Equation (4)
γ	[66.0 Pa K^{-1}, …., 68.5 Pa K^{-1}]	Equation (7)
Δ	[44.3 Pa K^{-1}, …., 392.2 Pa K^{-1}]	Equation (8)
β	[0.4168, …., 0.0489]	$\beta = 0.28\ \gamma/\Delta$
LE	[70.9 W m^{-2}, ..., 66.1 W m^{-2}]	$LE = R_n/(1+\beta)$
E_P	76.7 W m^{-2}	Searching for the maximum *LE* in *LE* estimates from previous step
T_s	287.7 K	Surface temperature corresponding to LE_{max} (or E_P)

References

Brutsaert, W.: On a derivable formula for long-wave radiation from clear skies. Water. Resour. Res., 11(5), 742-744, https://doi.org/10.1029/WR011i005p00742, 1975.

Hersbach, H., Bell, B., Berrisford, P., Hirahara, S., Horányi, A., Muñoz Sabater, J., et al.: The ERA5 global reanalysis. Q. J. R. Meteorol. Soc., 146, 1999-2049, https://doi.org/10.1002/qj.3803, 2020.

Kato, S., Rose, F.G., Rutan, D.A., Thorsen, T.J., Loeb, N.G., Doelling, D.R., et al.: Surface irradiances of edition 4.0 Clouds and the Earth' s Radiant Energy System (CERES) Energy Balanced and Filled (EBAF) data product. J. Clim., 31, 4501–4527, https://doi.org/10.1175/JCLI-D-17-0208.1, 2018.

Milly, P. C. D., and Dunne, K. A.: Potential evapotranspiration and continental drying, Nat. Clim. Change, 6, 946–949, http://dx.doi.org/10.1038/nclimate3046, 2016.

Rodell, M., Houser, P. R., Jambor, U. E. A., Gottschalck, J., Mitchell, K., Meng, C. J., et al.: The Global Land Data Assimilation System. Bull. Amer. Meteor. Soc., 85, 381– 394, https://doi:10.1175/BAMS-85-3-381, 2004.

Shakespeare, C. J., and Roderick, M. L.: The clear sky downwelling longwave radiation at the surface in current and future climates. Q. J. R. Meteorol. Soc., https://doi.org/10.1002/qj.4176, 2021.

Sheffield, J., Goteti, G., and Wood, E.F.: Development of a 50-year high-resolution global dataset of meteorological forcings for land surface modeling. J. Clim., 19, 3088–3111, https://doi.org/10.1175/JCLI3790.1, 2006.

Twine, T. E., Kustas, W. P., Norman, J. M., Cook, D. R., Houser, P. R., Meyers, T. P., et al.: Correcting eddy-covariance flux underestimates over a grassland, Agric. Forest. Meteorol., 103, 279 – 300, https://doi.org/10.1016/S0168-1923(00)00123-4, 2000.

Yang, Y., and Roderick, M. L.: Radiation, surface temperature and evaporation over wet surfaces, Q. J. R. Meteorol. Soc., 145, 1118–1129, https://doi.org/10.1002/qj.3481, 2019.